Design of an Automatic Power Quality Monitoring System by Using Integrated Approach

H.K. Siu and T.S. Chung
4/F., APB Centre, 9 Sung Ping Street, Hunghom,
Kowloon, Hong Kong

Abstract: The quality of electricity has been gaining more emphasis among utilities, service sectors and consumers. Good quality of electricity has to be maintained by strategic measures in coping with all sort of disturbances generated intrinsically in modern power electronic equipments and large commercial buildings. A means of improving electric power quality starts by a systematic identification of the power system disturbances which is posed to be a big challenge. The conventional approach based on Fourier Transform principles has its main drawback of losing the time-domain feature after transformation. In this context the technique of using wavelet transform appears to be more promising with its strength on handling signals on short time intervals for high frequency components and long time intervals for low frequency components. This study will propose a new approach called integrated approach by integrating the advantages of both Fourier and wavelet transforms. The wavelet transform is used to extract the required time-domain information from the high frequency components while the Fourier transform is used to provide the accurate measurement from the low frequency components. An automatic power quality monitoring system based on the integrated approach is then developed. Neural network classifier and adaptive neuro-fuzzy classifier are selected to implement the proposed approach of which its training and validation are performed via simulated data set and some real disturbance waveforms, respectively.

Key words: Power quality disturbances, fourier transform, wavelet transform, Multi-resolution Signal Decomposition (MSD), Neural network and Adaptive Neuro-fuzzy Inference System (ANFIS)

INTRODUCTION

Over the last two decades, emphasis on quality of electricity has attracted more and more attention to utilities, service sectors and bulk consumers. The concern of power quality has also deeply founded with users of modern power electronic equipment like those in commercial buildings which is sensitive to power system disturbances and/or those generated by itself. In order to monitor and control these disturbances so as to improve the electric power quality, these disturbances have to be identified and then analyzed. Therefore, the development of an automatic power quality monitoring system for the systematic identification of power system disturbances is essential and is posed to be a big challenge.

Primitively, the monitoring method is based on visual inspection on the disturbance waveform and then different typical monitoring devices, such as disturbance analyzers and harmonic analyzers, are developed in the industry. These analyzers usually employ techniques based on point-by-point comparison of the rms values of the distorted signal with its corresponding pure signal

and/or transformation of the data into the frequency domain via Fourier transform. However, the major problem of the traditional analyzing tools based on Fourier transform is that it will not provide sufficient information on the time domain. For non-stationary disturbances such as local transient signal, its location on the time axis will be lost after Fourier transform.

One technique emerged to overcome the above mentioned problem is by using wavelet transform whose strength is on handling signals on short time intervals for high frequency components and long time intervals for low frequency components. By means of the strength, wavelet transform is considered suitable for analyzing signals with localized impulses and oscillations particularly for those commonly present in fundamental and low order harmonics (Chul and Raj, 2000).

On the other hand, the Fourier transform still has its outstanding and well-proven performance on the measurement of the frequency spectrum of signals. In order to integrate the advantages of both transforms, a so-called "integrated approach" by using both Fourier and wavelet transforms is proposed in this study. This

Corresponding Author: H.K. Siu, 4/F., APB Centre, 9 Sung Ping Street, Hunghom, Kowloon, Hong Kong

study will also report on work regarding the development of neural network and adaptive neural-fuzzy classifiers for detecting and classifying the power system disturbances.

FOURIER AND WAVELET TRANSFORMS

Fourier transform: The Fourier Transform (FT), which breaks down a signal into constituent sinusoids of different frequencies, is perhaps the most well-known and reliable tool in signal analysis for many years. Mathematically, the FT is the sum over all time of signal x(t) multiplied by a complex exponential as below:

$$X(\omega) = \int_{-\infty}^{\infty} x(t)e^{-j\omega t} dt \qquad (1)$$

For a sampled signal, the Discrete Fourier Transform (DFT) is defined as: -

$$X(K) = \sum_{n=0}^{N-1} x(n)\exp(\frac{-j2\pi kn}{N}) \qquad (2)$$

Where x(n) is a sequence of samples from a continuous time signal x(t) taken every t seconds for N samples. If the samples are uniformly spaced, the Fourier matrix can be factored into a product of just a few sparse matrices and the resulting factors can be applied to a vector in a total of order N log(N) arithmetic operations. This is called Fast Fourier Transform (FFT).

However, the FT was developed based on assumption that the original time-domain function is periodic in nature. As a result, when dealing with functions with transient components that are localized in time, the FT cannot convey any time information about the transient components. In recent years, new families of orthonormal basis functions called "wavelets" have been emerged and new transforms have been developed to overcome the problem of the FT. (Mac, 1992).

Wavelet transform: Wavelet Transform (WT) employs a basis function called the mother wavelet, usually denoted by $\psi(t)$ which has a zero mean with sharp decays in an oscillatory fashion and effectively limited duration. Mathematically, the Continuous Wavelet Transform (CWT) of a given signal x(t) is generally defined as:-

$$CWT(a,b) = \frac{1}{\sqrt{a}} \int_{-\infty}^{\infty} x(t)\psi(\frac{t-b}{a})dt \qquad (3)$$

Where a is the dilation or scale factor, b is the translation factor and both variables are continuous

However, derivation of the CWT is quite time-consuming and computationally expensive and hence
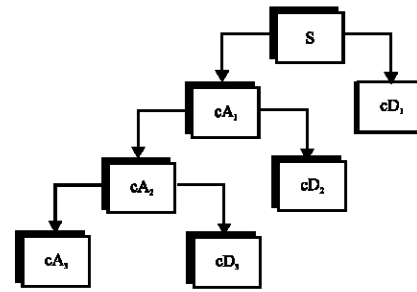

Fig. 1: MSD algorithm

ineffective in terms of computation time for deriving its information content. As an improvement, the Discrete Wavelet Transform (DWT) is developed by translating and dilating the mother wavelet discretely. The DWT is implemented by replacing a by a_o^m and b by $nb_o a_o^m$ in (3) and applying summation over the sample space as below:

$$DWT(m,n) = \frac{1}{\sqrt[m]{a_o}} \sum_k x(k)\psi(\frac{k - nb_o a_o^m}{a_o^m}) \qquad (4)$$

Where n represents the translation step and m represents the scaling step and is known as the level number. If $a_o=2$ and $b_0=1$, then the transform is known as the dyadic orthonormal wavelet transform (Alexander and Shaiq, 1998).

Multi-resolution signal decomposition: By using another basic function, namely scaling function $\phi(t)$, the dyadic orthonormal wavelet transform leads to an important technique called the Multi-resolution Signal Decomposition (MSD). The MSD technique enables a signal x(t) to be decomposed into a hierarchical set of scaling functions $\phi_{(j,k)}(t)$ or $\phi_l(t)$ with its approximation coefficients c(l) and shifted and dilated version of wavelet functions $\iota_{(j,k)}(t)$ with its detail coefficients d(j,k) by decomposing the approximation coefficients at each level to get further approximation and detailed coefficients (Fig. 1). Mathematically, the MSD technique can be described as: -

$$x(t) = \sum_{l \in z} c(l)\phi_l(t) + \sum_{j=0}^{j-1}\sum_{k \in z} d(j,k)\psi_{(j,k)}(t) \qquad (5)$$

Provided that each scaling and wavelet function shall have an orthogonal basis as illustrated below :-

$$\phi(t) = \sum_{k \in z} a_k \phi(2t - k) \qquad (6a)$$

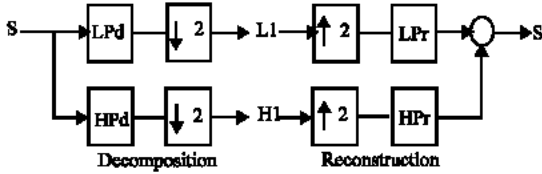$$\psi(t) = \sum_{k \in z} (-1)^k a_{k+1} \phi(2t - k) \qquad (6b)$$

Fig. 2: MSD by using filter banks

$$\varphi_{(j,k)}(t) = 2^{-j/2} \varphi(2^{-j}t - k); \; j,k \in z \qquad (7a)$$

$$\psi_{(j,k)}(t) = 2^{-j/2} \psi(2^{-j}t - k); \; j,k \in z \qquad (7b)$$

$$\sum_{k \in Z} a_{2k} = 1 \qquad (8a)$$

$$\sum_{k \in Z} a_{2k+1} = 1 \qquad (8b)$$

$$\sum_{k \in Z} a_k a_{k+2l} = 0 \; \text{ for } l \neq 0 \qquad (8c)$$

$$\sum_{k \in Z} \overline{a_k} a_k = 2 \qquad (8d)$$

Where j denotes scale or resolution index, k denotes translation location index and a_k are the scaling coefficients. Equation 8 list out the set of scaling conditions which must be satisfied before a set of a_k can be qualified as scaling coefficients (Mac, 1992).

In order to obtain the approximation and detail coefficients for each basis, we can take an inner product as given by:-

$$c(1) = <\varphi_1 \mid x> = \int x(t) \varphi_1(t) dt \qquad (9a)$$

$$d(j,k) = <\psi_{j,k} \mid x> = \int x(t) \psi_{(j,k)}(t) dt \qquad (9b)$$

Practically, the MSD is simulated by applying two-channel filter bank which is used to approximate the behavior of the wavelet transform. The signal will be decomposed with a high-pass filter and a low-pass filter as shown in Fig. 2. The low-frequency component usually contains most of the frequency of the signal, called the approximation, while the high-frequency component contains the details of the signal. Similarly, we can use reconstruction filter banks to reconstruct the discrete-time signal from the wavelet coefficients.

WAVELET ANALYSIS FOR POWER QUALITY

Detection of power quality disturbances: In Power Quality (PQ) disturbance signals, many disturbances contain sharp edges, transitions and jumps. As proposed by many authors, like Gaouda *et al.* (1999) we can use the MSD technique to discriminate the sharp edges, transitions and jumps contained in the detailed version from the smoothed version such that they can be
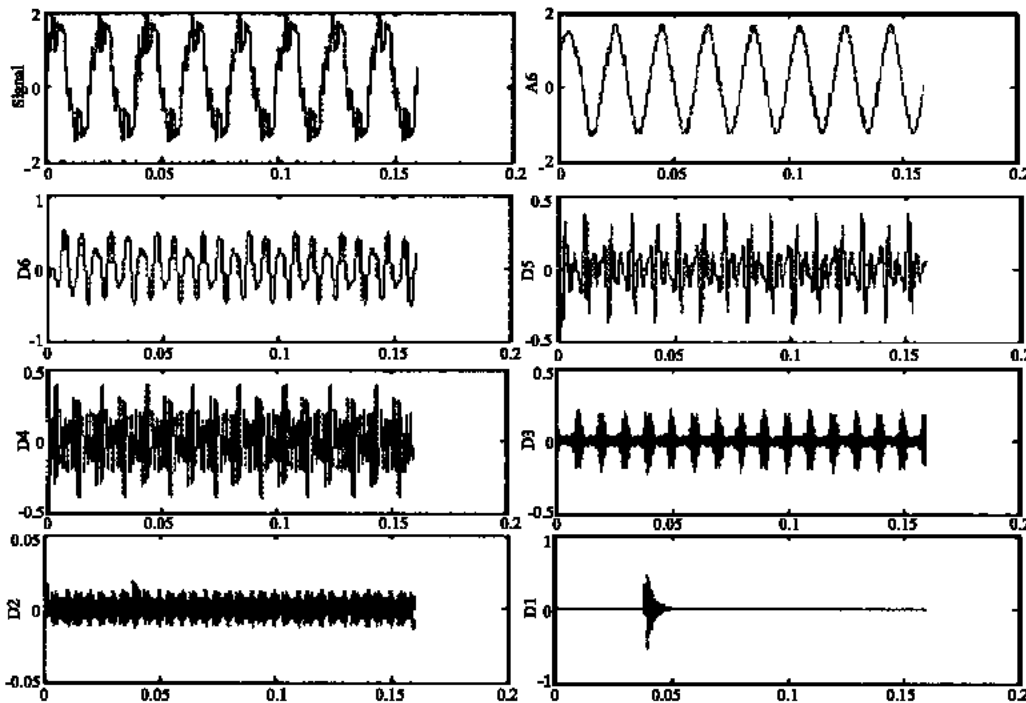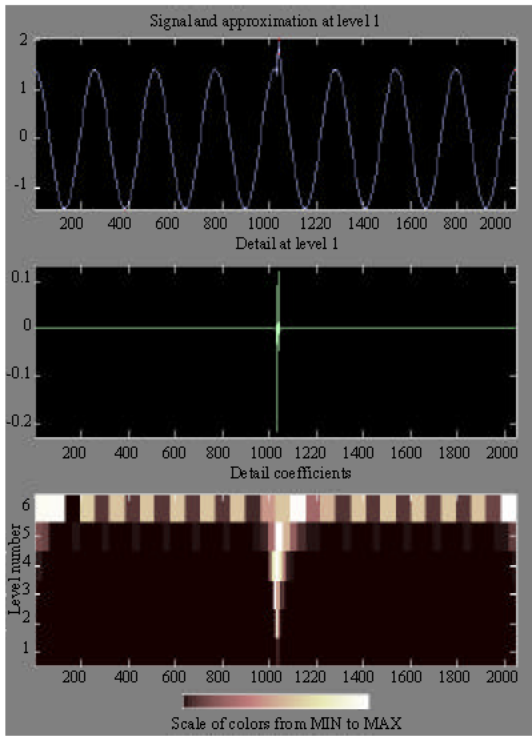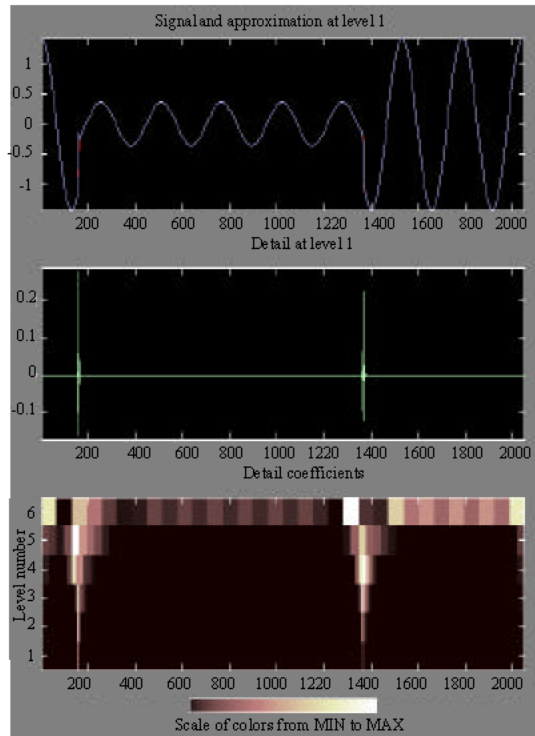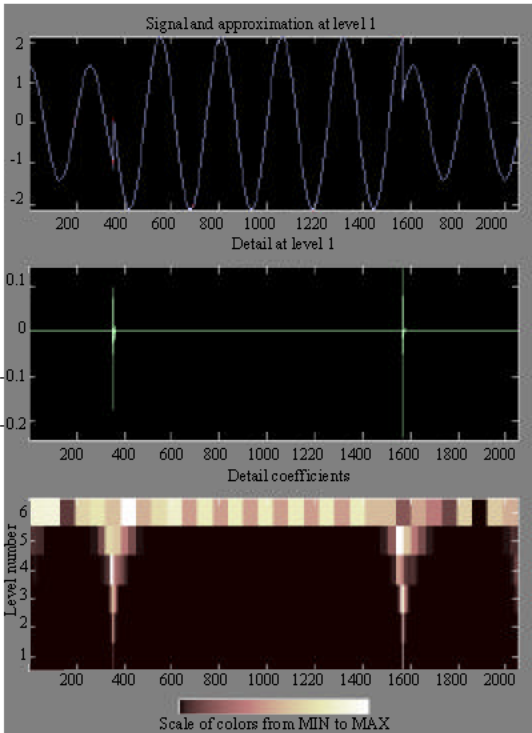

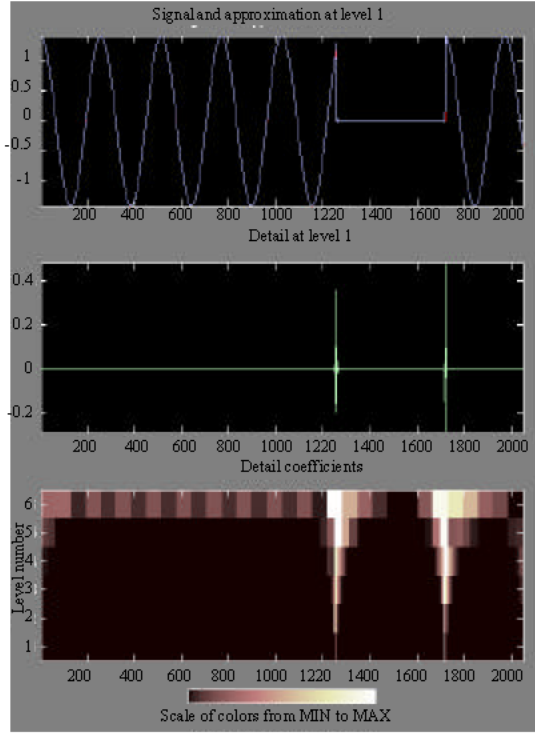Fig. 3: Six-level MSD of a distorted signal with transient and harmonics

(a) Impulse

(b) Voltage sag

(c) Voltage swell

(d) Interruption

(e) Harmonics
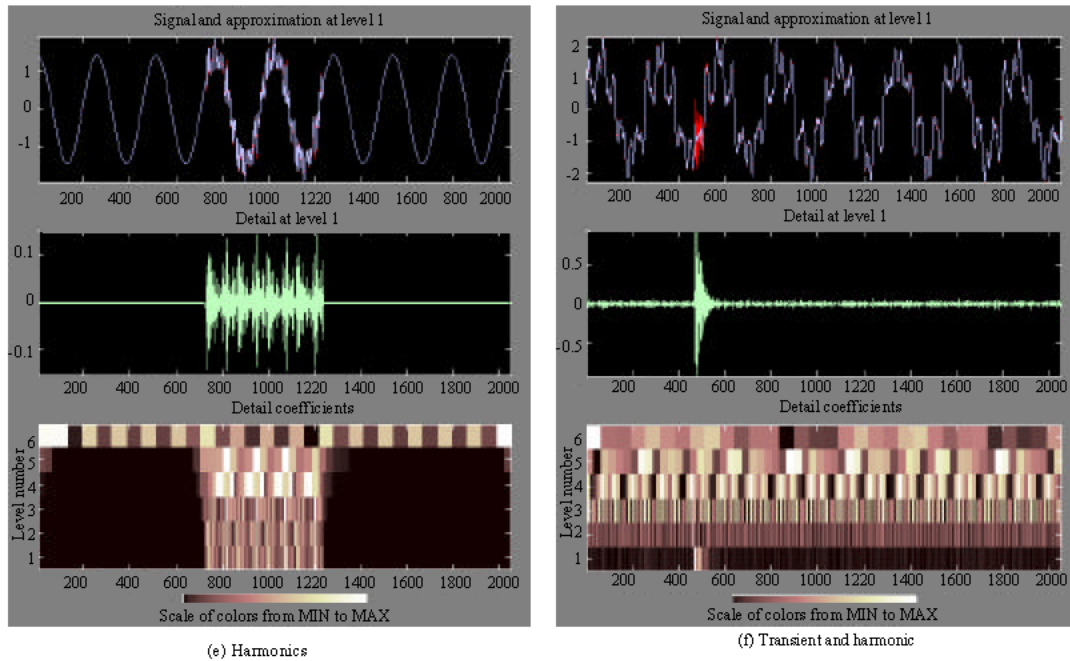

(f) Transient and harmonic

Fig. 4: Results of applying MSD to different PQ problems

analyzed separately. A typical example, a 6-level MSD of a distorted signal with transient and harmonics, is shown in Fig. 3. For other different PQ problems, e.g. impulse, voltage sag, voltage swell, interruption, harmonics and transient, etc., the results of applying MSD technique are quite promising as illustrated in Fig. 4.

Measurement of power quality disturbances: In order to obtain more information of the distorted signals for further analysis, such as trending analysis and rectification of the PQ problem, etc., the rms measurement of the distorted signals are required as defined:-

$$V_{rms} = \sqrt{\frac{1}{T}\int_0^T V^2 dt} \qquad (10)$$

According to Parseval's theorem, if any function x(t) can be presented as a series expansion by using a combination of the scaling functions and wavelets which form an orthonormal basis as shown in (5). Then

$$\int |x(t)|^2 dt = \sum_{i \in z} |c(1)|^2 + \sum_{j=0}^{J-1}\sum_{k \in z} |d(j,k)| \qquad (11)$$

Therefore, the energy of the distorted signal can be partitioned in terms of the approximation coefficients and

the detail coefficients at different resolution levels. (Gaouda *et al.*, 1999). Then the rms measurement of the distorted signal can be derived as follows:-

$$V_{rms} = \sqrt{\frac{1}{T}\sum_{1 \in z} c(1)^2 + \frac{1}{T}\sum_{j=0}^{j-1}\sum_{k \in z} d(j,k)^2} \qquad (12)$$

However, the decomposed waveform after MSD will provide non-uniform frequency bands that are in octave order. Hence, the MSD is not suitable to measure the rms values of individual harmonic components. Although Hamid *et al.* (2001) proposed to use the Wavelet Packet Transform (WPT) algorithm, which is a direct extension from the MSD algorithm to a full binary tree by decomposing both the detail and approximation coefficients to produce further coefficients, to overcome this limitation, errors still exist due to the roll-off characteristics of the selected wavelet.

Unlike the MSD algorithm, the conventional FT algorithm can decompose the signal into uniform frequency domain, so that the FT algorithm is suitable to measure the rms and power of individual harmonic components. Therefore, a so-called "integrated approach" using both the DWT and FFT algorithms is proposed in this study for resolving the problem.

AUTOMATIC POWER QUALITY MONITORING SYSTEM

Integrated approach: The so-called "integrated approach" will first decompose the distorted signal into two signals, i.e., detailed and smoothed/approximated versions, by using the DWT algorithm. The required time information such as the duration of the disturbance can now be extracted from the detailed version. The smoothed or approximated version will then be undergone the FFT algorithm in order to obtain the frequency spectrum of the distorted signal. This integrated approach is illustrated in Fig. 5.

An automatic power quality monitoring system is then developed based on the proposed integrated approach. Although application of wavelet analysis for recognizing PQ disturbances has been addressed on a number of cases, like Gaouda *et al.* (1999), Negnevitsky *et al.* (2000) and Santoso *et al.* (2000a, b) the proposed automatic power quality monitoring system carries unique features such as it can be used for both detection and rms measurement for the PQ disturbances at the same time.

Proposed classification procedures: According to the integrated approach, the proposed classification procedures are: -

Step 1: The input signal is firstly decomposed into the Detail coefficients (cD1) and the approximation coefficients (cA1) by using DWT.

Step 2: The input signal will be de-noised by applying threshold on the Detail coefficient (cD1).

Step 3: The Approximation coefficients (cA1) is transformed to frequency domain by using FFT after applying Hann window.

Step 4: Based on the result obtained after using FFT, the following features can be determined: -
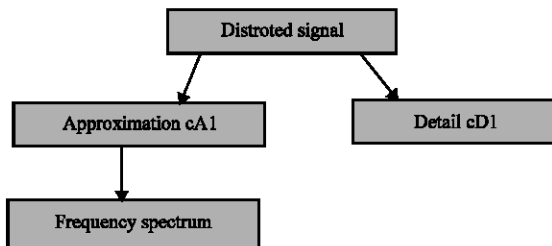

Fig. 5: Integrated approach by using both DWT and FFT algorithms

Table 1: List of different resolution levels (Sampling frequency = 12800 Hz)

Resolution level	Wavelet coefficients	Frequency band (Hz)	Central frequency (Hz)
1	cD1	6400-3200	4800
2	cD2	3200-1600	2400
3	cD3	1600-800	1200
4	cD4	800-400	600
5	cD5	400-200	300
6	cD6	200-100	150
7	cA6	100-DC	50

- DC component (V_{dc})
- Change of fundamental component (ΔV_1)
- Total Harmonic Distortion ratio (THD)
- Change of fundamental Frequency (ΔF)

Step 5: Based on the time information about the disturbances extracted from the de-noised Detail coefficients (cD1), we can measure: -

- Half-cycle rms value before transition (V_{rbs})
- Half-cycle rms value after transition (V_{rs})

Step 6: By applying MSD, the change of half-cycle spectrum of the input signal before and after transition (ΔP_{wc}) can be obtained and partitioned at different resolution levels (Table 1). And one more parameter (ΔV_{err}), i.e. the change of error between the measured rms value in Step 5 and by MSD technique to encounter the roll-off characteristics of wavelet, especially at the boundary frequency e.g., DC, 100, 200 and 400Hz, etc., will be also determined.

Step 7: The above extracted features will be passed to the classifiers for the identification of the disturbance.

One example containing transient, harmonics and noise to illustrate the principle of using "integrated approach" is shown in Fig. 6.

For Step 3, the accuracy of measuring the actual fundamental frequency and amplitude of discrete frequency components is enhanced by using Hann window and performing weighted average calculation.

For step 6, the adoption of MSD can achieve half-cycle decomposition which is the minimum duration of a voltage sag/swell, reduced number of multiplicative operations but lower accuracy when comparing with the similar operation of full-cycle decomposition by using FFT as proposed in my previous paper published (Siu and Ngan, 2004).

In this study, 2 classifiers called adaptive neuro-fuzzy classifier and neural network classifier will be employed to identify the nature of the disturbance.
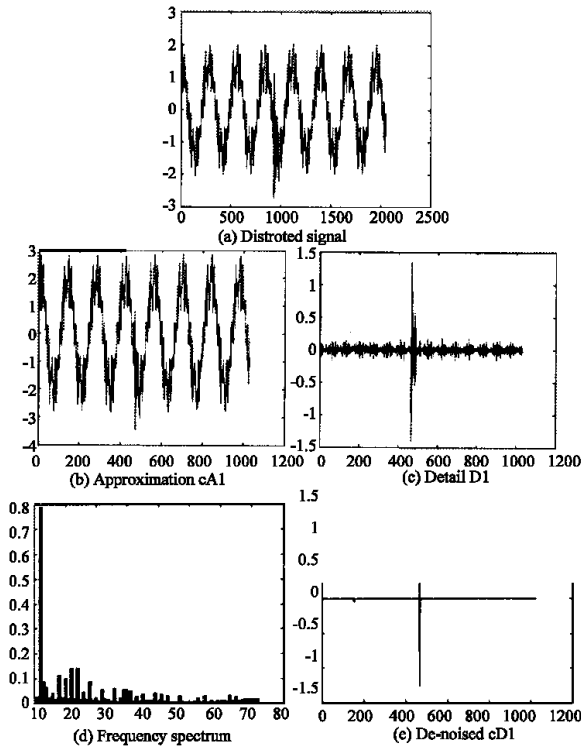
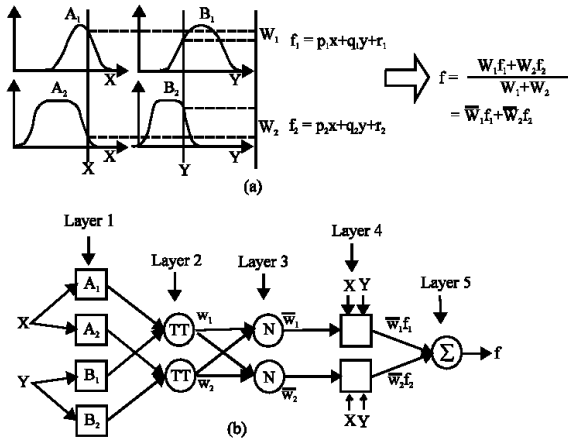Fig. 6: Example of using "integrated approach"

Fig. 7: Two-input first order Sugeno fuzzy model and the equivalent ANFIS architecture

Adaptive neuro-fuzzy classifier: Basically, the PQ disturbances can be divided into two categories, i.e., short duration variations and long duration variations. Referring to the features measured in Step 4, the following long duration variations can be readily identified according to the IEEE Std. 1159 (1995).

- Undervoltage (if -0.9 pu $< \Delta V_1 <$ -0.1 pu)
- Overvoltage (if 0.1 pu $< \Delta V_1$)

- Outage/Interruption (if $\Delta V_1 <$ -0.9 pu)
- DC offset (if $V_{dc} >$ threshold)
- Harmonics (if thd > threshold)
- Frequency variation (if abs(ΔF) > threshold)

Although the simple rule-based classifier can be constructed to identify the above PQ problems, a more accurate and flexible classifier, called adaptive neuro-fuzzy classifier, will be adopted in this study.

The adaptive neuro-fuzzy classifier will use an Adaptive Neuro-Fuzzy Inference System (ANFIS) based on Sugeno type system to classify the PQ disturbances as shown in Fig. 7. ANFIS is a class of adaptive network functionally equivalent to fuzzy inference system and is more suited to Sugeno inference system whose output membership functions are either linear or constant, i.e. first-order polynomial and whose overall output is obtained via "weighted average".

The ANFIS adopting some neuro-adaptive learning techniques provides a method for the fuzzy modeling procedure to learn information about a data set, in order to compute the membership function parameters that best allow the associated fuzzy inference system to track the given input/output data. The ANFIS proposed in this study will use a combination of least square estimation and back-propagation for membership function parameter estimation.

In order to classify the short duration variations, the characteristics of the disturbances are investigated via measuring and comparing the half-cycle spectrum before and after the transition of the disturbance by using MSD. The differences between two measured spectra against resolution level are plotted in Fig. 8.

For Fig. 8b-h, the resolution level no. 8 represents the error, ΔV_{err}, between the direct measured half rms valus and by MSD technique as mentioned in Step 6. When comparing with Fig. 8b and d, the change of spectra between impulse and transient is quite significantly different as the change of spectra for transient will contain high frequency components as shown in resolution level no. 3 in this example. Similarly, the change of energy spectra for voltage sag and swell can be readily identified as shown in Fig. 8f and h. Therefore, 2 Neural Network (NN) classifiers with the same structure (Fig. 9) are considered to memorize the pattern of the change of spectra for different short duration variations in order to implement the automatic PQ monitoring system.

Both neural network classifiers have 8 input neurons, i.e., ΔP_{we} and ΔV_{err}, 12 neurons in hidden layer and 2 output neurons, i.e. indicating impulse or transient for one classifier and sag or swell for another one. With the help
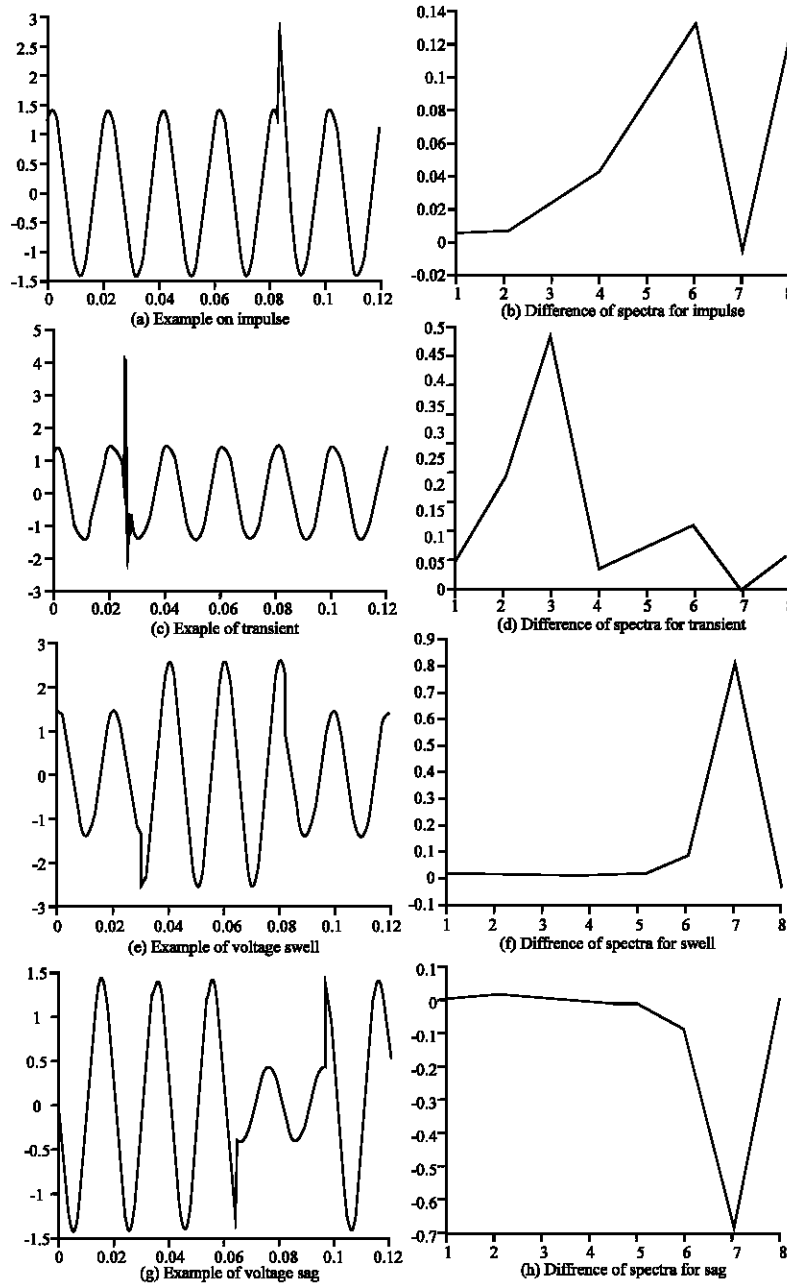
Fig. 8: Characteristics of short duration variations

of adaptive neuro-fuzzy classifier by incorporating the half-cycle rms values before and after the transition, i.e. V_{rps} and V_{rs}, we can even identify the start and end of the voltage sags/swells/interruptions as illustrated in Table 2.

Training and verification: In order to train the neural network classifier and adaptive neuro-fuzzy classifier, a set of simulated disturbance waveforms is generated as proposed by Liao *et al.* (2000) as listed in Table 3. After
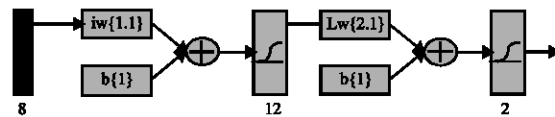
Fig. 9: Two-layer perceptron neural network classifier

passed the input features extracted from the generated waveforms of items (E), (F) and (G) and the corresponding

Table 2: Classification of Voltage Sag/Swell/Interruption

Type of disturbances	Half-cycle rms values	Output of NN classifier
(a) Start of Voltage Sag	0.1 pu <Vrs< 0.9 pu	Sag
(B) Start of Voltage Swell	1.1 pu <Vrs< 1.8 pu	Swell
(C) Start of Interruption	Vrs< 0.1 pu	Sag
(D) End of Voltage Sag	0.1 pu <Vrps< 0.9 pu	Swell
(E) End of Voltage Swell	1.1 pu <Vrps< 1.8 pu	Sag
(F) End of Interruption	Vrps< 0.1 pu	Swell

Table 3: Simulated waveforms generated for training

Simulated disturbances	No. of waveforms		
	0% Noise	0.5% Noise	1% Noise
(A) Overvoltage, undervoltage and outage	40	40	40
(B) DC offset	12	12	12
(C) Harmonics	21	21	21
(D) Frequency variation	27	27	27
(E) Impulsive transient	40	40	40
(F) Oscillatory transient	160	160	160
(G) Voltage sag, swell and Interruption	40	40	40
Total	1020		

Table 4: Results obtained from classifiers

	Signal A		Signal B	
(A) Undervoltage	-0.0021		1.0383	
(B) Overvoltage	-0.0018		-0.0001	
(C) Outage	-0.0021		-0.0015	
(D) DC offset	0		0	
(E) Harmonics	1	1		
(F) Frequency variation	0	0		
Time (s)	0.0259	0.0420	0.0262	0.0942
(G) Impulse	1	1	1	1
(H) Transient	0	0	0	0
(I) Start of Sag	0	0	0.6302	0
(J) Start of Swell	0.9856	0	0	0.0056
(K) Start of Interruption	0	0.0022	-0.0061	0
(L) End of Sag	-0.0017	0	0	1.046
(M) End of Swell	0	0.9068	0.0048	0
(N) End of Interruption	0	0	0	0.0002

target outputs to the neural network classifiers, the training result is plotted in Fig. 10. From Fig. 10, the error of classifier for impulse and transient dropped to 0.001667 after 64 epochs while the error of classifier for sag/swell has even dropped to 2.115×10^{-14} after 19 epochs.

At the same time, the extracted input features and the target outputs for items (A), (B), (C) and (D) and the outputs of the neural network classifier for sag/swell and the measured half cycle rms values for item (G) are also used to train up the adaptive neuro-fuzzy classifiers. After training, the performance of the trained adaptive neuro-fuzzy classifiers, i.e., surface plots of ANFIS, is shown in Fig. 11 for different type of PQ disturbances.

For verifying the performance of the classifiers in real situation, I have downloaded the test waveforms published by IEEE 1159.2 Working Group. Two sampled waveforms containing voltage swell and voltage sag are presented as shown in Fig. 12. The results obtained from the classifiers are listed in Table 4.

For Signal A, the start of voltage swell was recognized at time = 0.0259s while the end of voltage swell was recognized at time = 0.0420s. Hence, the duration of the voltage swell was about 0.0420s-0.0259s = 0.0161s. Impulses and harmonics were also identified. The indication of containing harmonics may be due to the highly distorted waveform. As a result, the Signal A was identified containing harmonics, impulses and voltage swell which generally matched the actual observation.

For Signal B, the start of voltage sag was recognized at time = 0.0262s while the end of voltage sag was recognized at time = 0.0942s. Hence, the duration of the voltage sag was about 0.0942s-0.0262s = 0.0680s and the overall voltage was also reduced such that undervoltage was identified. Similarly, impulses and harmonics were also recognized. The indication of containing DC component may be due to the highly non-symmetrical waveform of the signal. As a result, the Signal B was identified containing
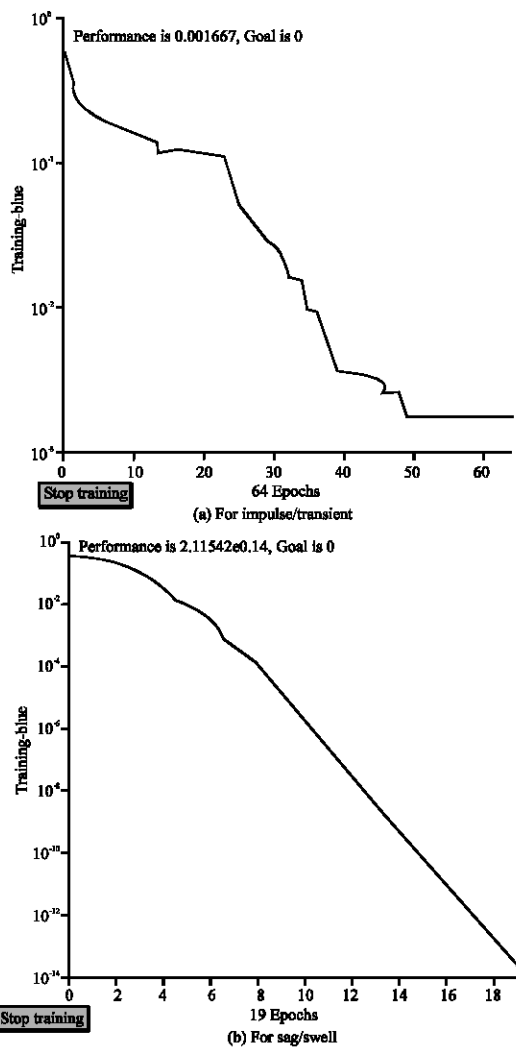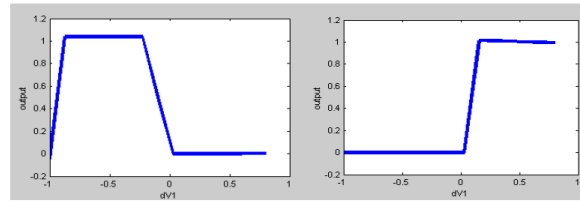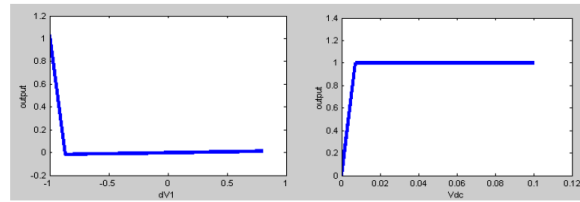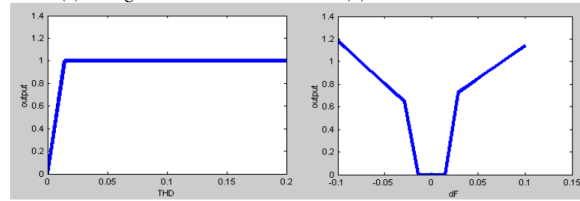

Fig. 10: Plot of error of neural network classifiers
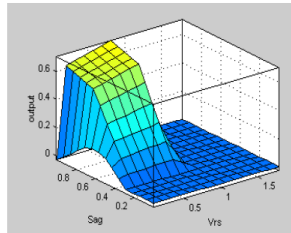
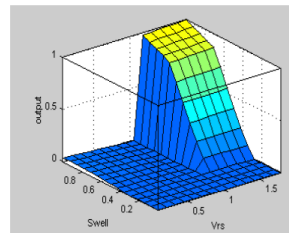(a) Undervoltage   (b) Overvoltage
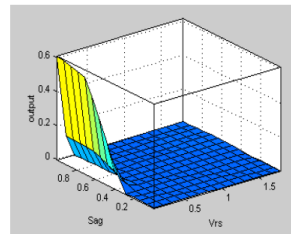
(c) Outage   (d) DC offset

(e) Harmonics   (f) Frequency variation
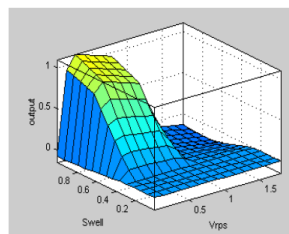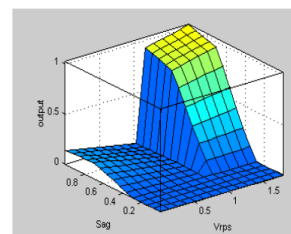
(g) Strat of voltage   (h) Strat of voltage swell
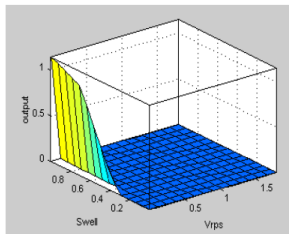
(i) Strat of interruption   (j) End of voltage sag

(k) End of voltage swell   (l) End of interruption

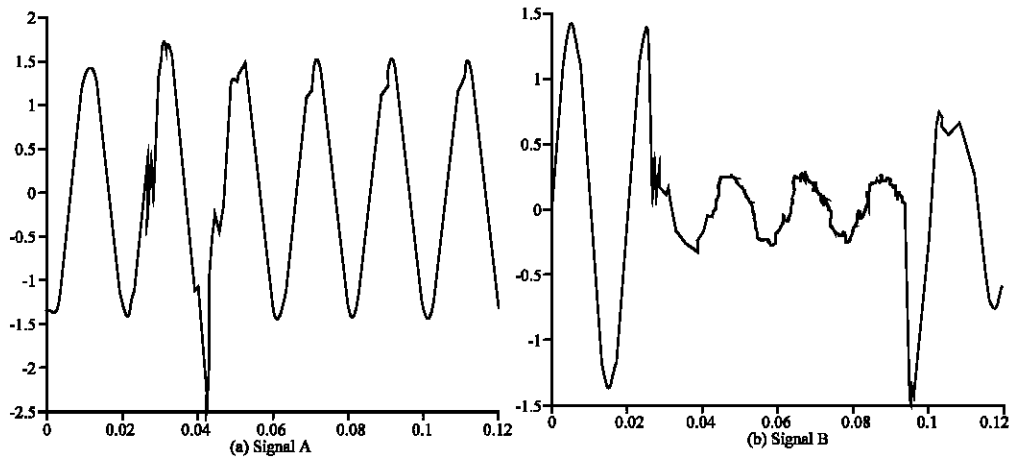Fig. 11: Surface plots of trained ANFIS

Fig. 12: Two sampled signals containing voltage swell and sag

undervoltage, DC offset, harmonics, impulses and voltage sags that generally matched the actual observation.

As revealed in Table 4, all the voltage sag and swell including the start time and end time could be recognized accordingly. The impulses, harmonics and dc offset could be identified as expected. Hence, the overall performance of the trained neural network classifiers and adaptive neuro-fuzzy classifiers was quite satisfactory and promising.

FUTURE WORK

By using integrated approach, the rms measurement of voltage is readily available. After passing through the classifiers, the characteristics of the power quality disturbances can be easily extracted. Just by applying FFT on current waveform, the rms measurement of current and the corresponding power measurement can be also obtained. Hence, an effective power quality monitoring database, which will consist of the rms and power measurements of both voltage and current and the characteristics of the power quality disturbances detected, can be set up to monitor the power quality condition such that we can implement predictive maintenance and energy management of electrical system in future.

CONCLUSION

In short, an automatic power quality monitoring system is developed by using the proposed integrated approach, i.e. by using DWT and FFT. This system can perform both the extraction of the required time information and the rms measurement of the distorted

signal. Two classifiers, namely adaptive neural-fuzzy classifier and neural network classifier, are suggested and trained by a set of simulated disturbance waveforms. Their performance is then verified via some real disturbance waveforms. Although the test results of the proposed automatic power quality monitoring system are quite promising, the real-life power quality disturbance data will not be as simple as those simulated waveforms and the size of sampled waveforms is hard to be sufficiently large. Therefore, further adjustment and modification is required before this proposed automatic power quality monitoring system can be applied in real-life situation. In future, the system can be adjusted and modified by gathering more and more real disturbance waveforms in order to increase its accuracy. Software to analyze and keep track of the power quality monitoring database can be developed such that practical applications like predictive maintenance and energy management of electrical system can be carried out in future.

REFERENCES

Alexander Domijan and Muhammad Shaiq, 1998. A New Criterion Based on the Wavelet Transform for Power Quality Studies and Waveform Feature Localization, ASHRAE. Trans. Res., pp: 3-16.

Chul Hwan Kim and Raj Aggarwal, 2000. Wavelet transforms in power systems-Part 1: General introduction to the wavelet transforms, Power Eng. J., pp: 81-87.

Effrina Yanti Hamid, Zen-Ichiro Kawasaki and Redy Mardiana, Wavelet Packet Transform for Rms and Power Measurements in 2001 IEEE. Power Eng. Soc. Summer Meeting, 2: 1243-1245.

Gaouda, A.M., M.M.A. Salama, M.K. Sultan and A.Y. Chikhani, Power Quality Detection and Classification Using Wavelet-Multiresolution Signal Decomposition, IEEE. Trans. Power Delivery, 14: 1469-1476.

IEEE Recommended Practices for Monitoring Electric Power Quality, 1995. IEEE. Standard, pp: 1159-1995.

Jiansheng Huang, Michael Negnevitsky and D. Thong Nguyen, 2002. A Neural-Fuzzy Classifier for Recognition of Power Quality Disturbances, IEEE. Trans. Power Delivery, 17: 609-616.

Kezunovic, M. and Y. Liao, 2000. A novel method for equipment sensitivity study during power quality events, In: Proc. IEEE. Power Eng. Soc. Winter Meeting, Singapore, pp: 230-235.

Mac A. Cody, 1992. The Fast Wavelet Transform Beyond Fourier Transforms, Dr. Dobb's J.

Siu, H.K. and H.W. Ngan, Automatic Power Quality Recognition System using Wavelet Analysis, in Proc. IEEE Int. Conf. Electric Utility Deregulation, Restructuring and Power Technol., 2004 (DRPT2004), Hong Kong, IX.Biographies, 1: 311-316.

Surya Santoso, Edward J. Powers, W. Mack Grady and Antony C. Parsons, 2000. Power Quality Disturbance Waveform Recognition Using Wavelet-Based Neural Classifier-Part 1: Theoretical Foundation, IEEE. Trans. Power Delivery, 15: 222-228.